Available online at www.sciencedirect.com

ScienceDirect

Procedia Manufacturing 10 (2017) 923 – 934

Procedia MANUFACTURING

45th SME North American Manufacturing Research Conference, NAMRC 45, LA, USA

Design optimization of plastic injection tooling for additive manufacturing

Tong Wu[a], Suchana A. Jahan[a], Yi Zhang[a], Jing Zhang[a], Hazim Elmounayri[a*] and Andres Tovar[a]

[a]*Mechanical Engineering, Indiana University-Purdue University Indianapolis, IN, 46202, U.S.*
**Corresponding author helmouna@iupui.edu*

Abstract

This work presents a systematic and practical finite element based design optimization approach for the injection tooling adaptive to additive manufacturing (AM) technology using stereo-lithography (SLA) and powder bed fusion (PBF). First a thermomechanical optimization of conformal cooling is implemented to obtain the optimal parameters associated with conformal cooling design. Then, a multiscale thermomechanical topology optimization is implemented to obtain a lightweight lattice injection tooling without compromising the thermal and mechanical performance. The design approach is implemented to optimize a real design mold and the final optimal design is prototyped in SLA and the manufacturability in PBF has been discussed.

Peer-review under responsibility of the organizing committee of the 45th SME North American Manufacturing Research Conference

Keywords: injection tooling; conformal cooling optimization; topology optimization; additive manufacturing

1. Introduction

The creation of production tools for prototype and production components represents one of the most time consuming and costly phases in the development of new products. To reduce the manufacturing lead-times and cost, prototyping and manufacturing processes has already been rapidly developed and integrated to the manufacturing progress. One of the important applications of prototyping and manufacturing processes is to product injection tooling. Based on current additive manufacturing (AM) technologies, up to 50% in time and cost in tooling production can be saved [1]. The outstanding advantage of using AM to fabricate injection tooling is the effectiveness to obtain complicate geometries of the master pattern and its conformal cooling channels. Furthermore, the utilization of AM offers an opportunity to produce lighter and more efficient molds and dies composed of lattice structure that saving the material used in AM process. With the development of finite-element based structural

Peer-review under responsibility of the organizing committee of the 45th SME North American Manufacturing Research Conference
doi:10.1016/j.promfg.2017.07.082

optimization methods, it is possible to improve the design of today's injection tooling and create lightweight, complex designs with higher thermomechanical performance.

In the earlier work [2], we propose a framework for optimizing the design of Injection tooling with conformal cooling for additive manufacturing. In this study, we improve this concept to develop a finite element based approach to find the optimal parameters for the conformal cooling channels, as well as optimal functionally graded lattice unit cell distribution of the mold body. To achieve this, thermomechanical optimization problems associated with design geometrical parameters are formulated. The optimal design parameters can be obtained by using derivative-free optimization solvers. Then, the design domain of the mold with optimal conformal cooling is optimized to a structure composed of solid and lattice phases of unit cells. The manufacturability of the final optimal structures are discussed and will be demonstrated in the future work.

This work is presented in next sections. First, a literature review about is presented in section 2. In section 3, the procedure of thermomechanical conformal cooling for a real injection tooling is described. Section 4 presents the proposed multiscale thermomechanical topology optimization for this injection tooling. Section 5 shows the design prototype and the discussion of manufacturability. Finally, in section 6 conclusion are given.

2. Literature review

2.1. Thermomechanical optimization of conformal cooling

Conformal cooling is defined as the cooling channels that conform to the surface of the mold core (or cavity) for efficiently transferring the heat from the mold core to the coolant channels, aiming to maintain a steady and uniform cooling performance for the molding part [3]. Compared with conventional cooling, conformal cooling can often result in reduction of production cycle time, warpage and shrinkage, which in turn may provide financial benefit to industries. Nowadays, the unique capabilities of AM technologies allow an innovative design approach that challenges traditional guidelines of the plastics injection molding industry. Research has indicated significant advantages of AM generated, highly complex conformal cooling channels. In research, computer generated molds designed with conformal cooling channels have exhibited increased thermal and mechanical performance and indicate a reduction of material and manufacturing costs. The optimization of these conformal cooling channels can be considered a finite element-based parametric task, with optimal parameters obtained using either of Design of Experiment (DoE) or non-gradient based optimization algorithm. Choi et al employed a commercial process integration and design optimization tool called Process Integration, Automation and Optimization (PIAnO) to perform parametric study for mold cooling optimization [4]. Ramos et al propose a multi-objective genetic algorithm called NSGA-II to obtain the optimal parameters in the optimal mold design [5]. Simulations have shown that these designs have reduced cooling time, improved temperature uniformity and reduced volumetric shrinkage. However, these optimizations have lack adequate stiffness to ensure structural stability of the injection mold. An injection mold is also subjected to high levels of pressure from the heat polymer melt as well as clamping force, which may be arising high von Mises stress and deflection on the surface of the molds and pipes. In this study, a thermomechanical optimization is implemented to obtain not only an optimal design has both thermal performance, but also a design enables to withstanding pressure mechanical loads and thermal expansion during the injection molding cycle.

2.2. Multiscale thermomechanical topology optimization

Among currently available finite element-based design methods, topology optimization is recognized to provide innovative, high-performance layouts that are suitable to AM. Integral to the proposed design process is the use of multiscale thermomechanical analysis for mechanical and thermal properties. The term multiscale refers to two length scales: mesoscale and macroscale. Mesoscale refers to the length of a unit cell. At the mesoscale, lattice unit cells are analyzed in order to derive homogenized thermal and mechanical properties as a function of their relative density. These homogenized properties are derived from asymptotic homogenization methods [6]. The shape of the materials is regular and controlled by a few of geometric parameters that define a potentially large range porosity. The material interpolation is modified to guide a macroscale structure consisting of only the discrete set of a priori

set of given unit cells. These given unit cells are optimally distributed to form a multiphase lattice structure by solving thermomechanical topology optimization problem.

With respect to thermomechanical analysis, mechanical topology optimization with the consideration of thermal expansion has been used in the micro-electro-mechanical-systems (MEMS) [7]. Topology optimization with reference to heat conduction has been employed to minimize the temperature gradient magnitude distribution (heat dissipation) for thermal components including heat sinks for multichip modules [8]. Studies that consider coupled heat conduction and linear elasticity in the topology optimization have been proposed in our previous work [2]; however, the studies are limited to 2D solid-void structures.

2.3. Additive manufacturing using Powder bed fusion

Powder bed fusion (PBF) is one of the most commonly used technologies for additive manufacturing of metals. In this PBF manufacturing process, a power source (laser of electron beam) selectively melt the powder bed to form a thin solid layer, therefore a 3D object is fabricated layer-by-layer. Based on type of power sources, PBF can be further divided into two categories: the selectivity laser melting (SLM) and the electron beam melting (EBM) [9]. The SLM process uses laser as energy source, the movement of laser is controlled by mirror reflection. Powder is moved from powder tank to the building platform by a blade or brush. In the EBM process, electron beam is used for the energy source. Powder is stored in hoppers, in the recoating process, powder is firstly dumped onto the sides of building platform, and then it is recoated by a rake. During the PBF processes, localized temperature often reach the melting or boiling points of the powder metal, so that the materials subject to rapidly melting and solidification in few microseconds. Thus, the complicity of the thermal history leads to a unique columnar-grained microstructure [10]. Consequently, the anisotropy of the PBF fabricated material usually show anisotropic mechanical properties, including elastic modulus, yield strength and ultimate strength [11].

3. Thermomechanical optimization of conformal cooling

This section presents the procedure of purposed FEA based thermomechanical optimization applied to a real injection mold example. The FEA problem is solved in commercial software COMSOL Multiphysics. The relations between the mold geometries and their finite element models are treated as black box functions, the optimal solutions of which are required to be solved using derivative free optimization methods. Among many methods, three methods are used to solve this problem in this study, namely Nelder-mead simplex, constrained optimization by linear approximation (COBYLA) and are Genetic Algorithm (GA). Nelder-mead and COBYLA are two solvers available in COMSOL Multiphysics. In Nelder-mead method, the design variables walk toward the values that can improve objective function value by iteratively replacing the worst corner of a simplex in the control variable space, the details can be seen in [12]. COBYLA solves a sequence of linear approximations constructed from objective and constraint values sampled at the corners of a simplex in control variable space, the details can be seen in [13]. These two methods are computationally cheap, but there is a high possibility that a local minimum is found. Thus, Genetic algorithm (GA), which has been reported to have a high possibility to find a global optimum [5], is applied as well.

The mold is utilized for producing bump caps used in the car shock absorber. The mold contains a cavity plate and a core plate, both of them are made of stainless steel. In the following simulations in section three and four,

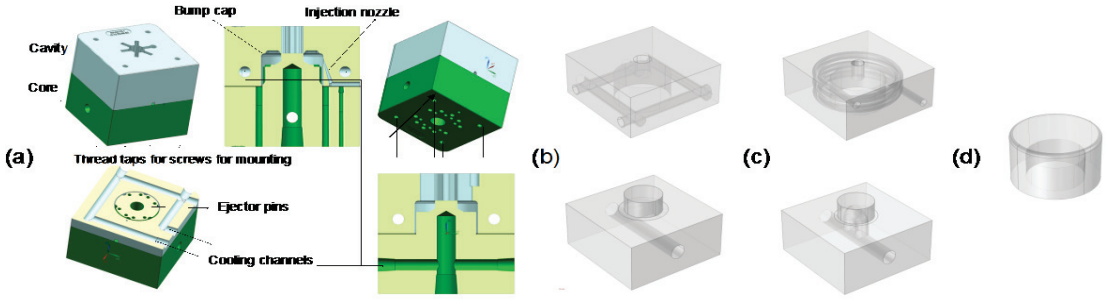

Fig. 1.: (a) the configuration of the injection mold; (b) simplified design domains for conventional cooling analysis; (c) Simplified design domains for conformal cooling analysis; (d) simplified domain of injected part.

empirical properties for 3D-printed A286 stainless steel are used: density ρ_0=7850kg/m3, Young's Modulus E=200GPa, Poisson ratio ϑ=0.3, thermal conductivity k=17.8 W/ (m·K). The conventional cooling channels for both plates are straightly drilled due to the limitation of machining technique. With additive manufacturing, this limitation can be overcome, therefore conformal cooling channels are free to design. Considering the geometries of the bump cap, the location of the injection nozzle, ejector pins, bolts etc., the general design of the conformal cooling including a helix channel for the cavity and a U-shape channel for the core (Fig. 1 (a)). To reduce computation load, simplified design domain for conventional cooling and conformal cooling are established (Fig. 1(b) and (c)). The performance of optimal model will be evaluated through a comparative study. Parameter optimizations are subsequently implemented for both the cavity and core based on static state thermal and structural FEA. Geometry constraints, physics constraints and objectives will be described. Transient state analysis are performed for the conventional and conformal cooling channel designs to evaluate the effect of the optimization.

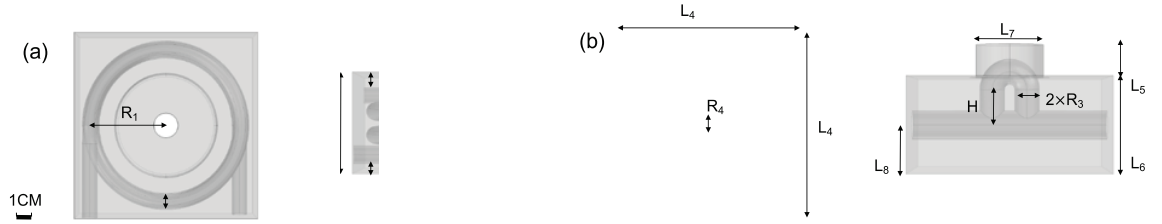

Fig. 2.: Geometry of (a) cavity plate, three design variables are included, namely the major radius of the helix R_1, the minor radius of the helix R_2, and the axial pitch P; (b) core plate, three design variables are included, namely the radius of vertical pipe R_3 , the half of the distance between two vertical pipes R_4, height from the straight pipe to the U-shape pipe's bottom H.

3.1. Geometry constraints

For the cavity, the general conformal cooling design consists of a helix channel and two straight channels connecting this helix (Fig.2 (a)). The unchanged parameters are L_1 =12.446cm, L_2 = 7.0120cm, and L_3 =5.4864cm. Besides, r=0.25cm is defined as the minimal reserved thickness between any of two surfaces, n =2.5 is the number of turns for the helix. Three parameters associated with the helix channel are required to be

optimized, which are the major radius R_1 , minor radius R_2 and the pitch distance P . These three parameters satisfy the following geometric constraints:

$$\begin{gathered} n \times P + 2 \times R_2 \le L_3 - 2 * r \\ P = \max(r + 2 \times R_2, P) \\ 0.5 \times L_2 + R_2 + r \le R_1 \le 0.5 \times L_1 - R_2 - r \\ P, R_1, R_2 \ge 0, \end{gathered} \tag{1}$$

where the first row enables the helix properly fixed within the cavity height, the second row controls the real pitch distance, the third row enables the helix located within the cavity with minimum reserved thickness between any of two surfaces.

For the core, the general conformal cooling design consists of a straight channel and a U-shape channel. The dimension of the cavity plate is L_4=12.446cm, L_5 =2.0320cm and L_6 =5.7404cm. Besides, L_7=4.3002cm and L_8=2.7980cm. Three parameters associated with the U-shape channel are required to be optimized, which include: R_3, the radius of vertical pipe; R_4, half of the distance between two vertical pipes, and H, the height from the straight pipe to the U-shape pipe's bottom (Fig. 2 (b)). These three parameters satisfy the following geometric constraints:

$$\begin{gathered} 2 \times R_3 + R_4 + H + L_8 + r \le L_5 + L_6 \\ 2 \times (R_3 + R_4) \le L_7 - 2 \times r \\ R_4 - R_3 \ge 0.5 \times r \\ H, R_3, R_4 \ge 0, \end{gathered} \tag{2}$$

where the first two rows enable the U-shape pipe fixed within the core insert, the third row maintains a minimal thickness between two vertical branches of the U-shape pipe.

3.2. Physics objectives and constraints

The top surface of the cavity plate sustains a uniformly distributed clamping load of -1.08KN in z-direction, and injection pressure on the cavity is 131 MPa. Rollers are applied on the lateral surface nodes. The nodal displacement of the bottom surface is constrained in the z-direction (Fig. 3). The temperature of cooling channel surface is 299.85 K (26.7°C). A heat flux of 200 W is imposed on the cavity. All other surfaces are insulated (Fig. 4).

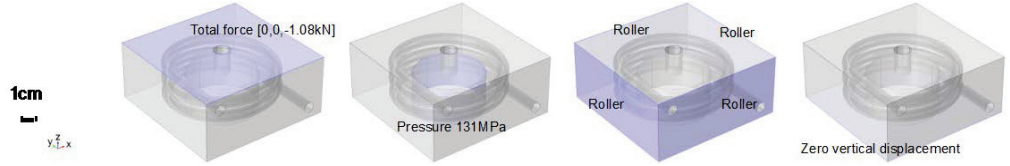

Fig. 3**:** mechanical load and boundary conditions for the cavity plate.

The thermal FEA model shows, the temperature variation of the injected part surface is small with the helix design (less than 0.1K), hence the objective is chosen to minimize the maximum temperature at the surface in contact with the injected bump cap. Γ_1 :

$$\min T^1_{max} \text{ on } \Gamma_1 , \tag{3}$$

and the maximum von Mises stress σ^1_{max} of the pipe surface S_1 should below the allowed stress σ_{limit} =350MPa in this study:

$$\sigma^1_{max} - \sigma_{limit} \le 0 \quad \text{on } S_1. \tag{4}$$

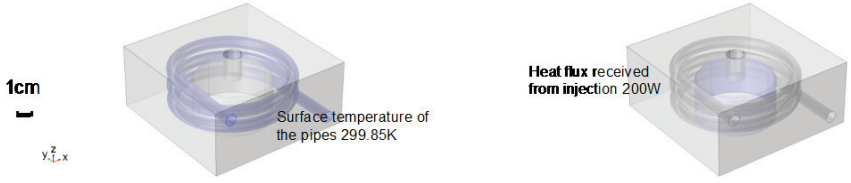

Fig. 4: thermal heat flux and boundary conditions for the cavity plate.

Finally, the problem statement is:

$$\begin{gathered}\text{Find } R_1, R_2, P \\ \text{Min Eq. (3)} \\ \text{Subject to Eq. (1) and Eq. (4).}\end{gathered} \tag{5}$$

In the constraints, the design variable in Eq. (1) can be directly sampled, thus only the conditions satisfying Eq. (1) will be computed, but the value of Eq. (4) only can be evaluated from FEA result of current iteration. Since Eq. (3) and (4) are evaluated simultaneously, the problem can be reformulated as:

$$\begin{gathered}\text{Find } R_1, R_2, P \\ \text{Min Eq. (3)}+p_1(\sigma_{max} - \sigma_{limit}) \\ \text{Subject to Eq. (1),}\end{gathered} \tag{6}$$

where p_1=10 is defined as the external penalty factor. This penalty number avoids the $\sigma_{max} \geq \sigma_{limit}$ when the objective minimum is achieved.

The bottom surface of the core plate sustains a uniformly distributed clamping load of 1.08KN in z-direction, and injection pressure on the core insert is 131 MPa. Rollers are applied on the lateral surface nodes. The nodal displacement of the top surface is constrained in the z-direction (Fig. 5). The temperature of cooling channel surface is 299.85 K (26.7°C). A heat flux of 200 W is imposed on the core. All other surfaces are insulated (Fig. 6).

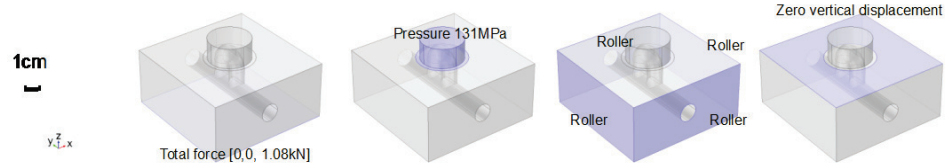

Fig. 5: mechanical load and boundary conditions for the core plate.

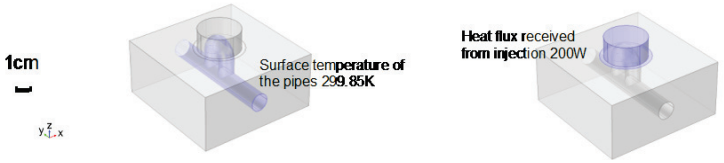

Fig. 6: thermal heat flux and boundary conditions for the core plate.

Modelling of optimization problem for the core is similar with the problem statement for the cavity. The thermal FEA model shows, the temperature variation of the injected part surface is small with the U-shape design (less than 0.15K), hence the objective is chosen to minimize the maximum temperature at the surface in contact with the injected bump cap Γ_2:

$$\min T_{max}^2 \text{ on } \Gamma_2, \tag{7}$$

and the maximum von Mises stress σ_{max}^2 of the pipe surface S_2 should below the allowed stress σ_{limit} (350 MPa):

$$\sigma_{max}^2 - \sigma_{limit} \leq 0 \quad \text{on } S_2, \tag{8}$$

Finally, the problem statement is

$$\begin{gathered}\text{Find } D, H, R \\ \text{Min Eq. (7)} \\ \text{Subject to Eq. (2) and Eq. (8).}\end{gathered} \tag{9}$$

Similarly, the problem can be reformulated as:

$$\begin{gathered}\text{Find } D, H, R \\ \text{Min Eq. (7)} + p_2(\sigma_{max} - \sigma_{limit}) \\ \text{Subject to Eq. (2),}\end{gathered} \tag{10}$$

where p_2=10 is defined as the external penalty factor.

3.3. Optimization result and testing in transient analysis

The resulting optimal parameters and corresponding σ_{max} and T_{max} are shown in Table 1 and Table 2. With Nelder-Mead method, the constraint of σ_{max} is slightly violated with the application of external penalty numbers p_1=p_2=10. In fact, the objective values derived by Nelder-Mead method from Eq. (6) and Eq. (10) are higher than those derived by GA method. This implies Nelder-Mead method leads a local optimum. Similar results are found when COBYLA method is applied. Since there are no guidelines are found to determine the best value of external penalty numbers for this problem, we prefer GA method among these three methods. The results derived from GA are adopted and used in the further thermomechanical topology optimization.

Table 1. The optimal parameters and corresponding σ_{max} and T_{max} for the cavity

METHOD	$R_1(cm)$	$R_2(cm)$	P(cm)	$\sigma_{max}(Mpa)$	$T_{max}(K)$
NELDER_MEAD	4.4046	0.4526	1.4952	350.10	325.35
COBYLA	4.3116	0.4391	1.4970	358.51	324.88
GA	4.8056	0.4828	1.3583	343.32	328.16

Table 2. The optimal parameters and corresponding σ_{max} and T_{max} for the core

METHOD	D(cm)	H(cm)	R(cm)	$\sigma_{max}(Mpa)$	$T_{max}(K)$
NELDER_MEAD	0.8801	2.5781	0.5847	390.28	375.67
COBYLA	1.3914	2.8026	0.5133	331.79	383.28
GA	1.1160	2.1973	0.7889	288.33	381.44

Transient analysis for the original design and optimal design are implemented to evaluate the cooling time improvement of the conformal cooling design. Assume the initial temperature of melting plastic is 473.15 K (200℃), the initial temperature of the mold is 343.15 K (70℃), the inlet water velocity for both cavity and core is 1 m/s. The volume of the injected part is 100.4 cm^3. The injected part is made of polyurethane, which has thermal conductivity 0.32 W/ (m· K), density 1250 kg/m^3, and heat capacity 1540 J/ (kg· K). Assume the Churchill friction model is used, and the surface of roughness factor is 0.046mm. The average temperature of plastic part over 300 seconds is shown in Fig. 7 (a) and the average temperature of the injection mold is shown in Fig.7 (b). Compare to the original design, the optimal conformal cooling reduce 9.62 K temperature for plastic part and 2.94 K temperature for the injection mold, which can be concluded as a significant improvement [14].

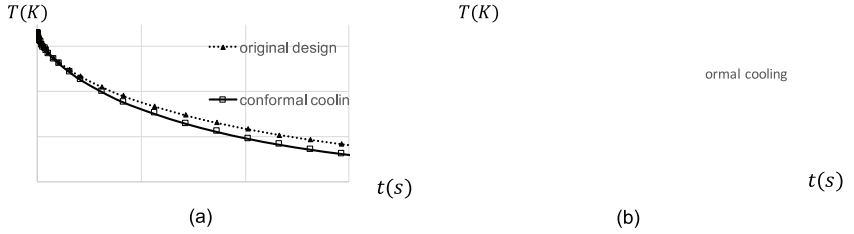

Fig. 7: (a) the average temperature of plastic part over 300 seconds, and (b) the average temperature of the injection mold.

4. Multiscale thermomechanical topology optimization

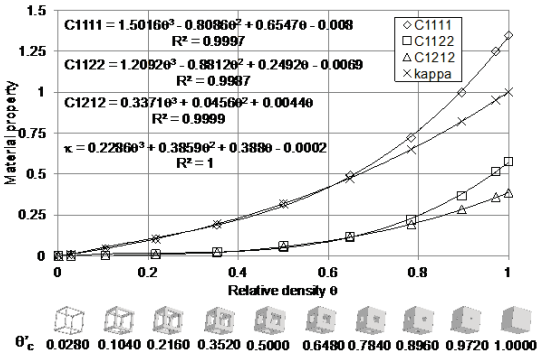

Fig. 8: interpolation of elasticity coefficients and thermal conductivity for 3D unit cells.

After the determination of the optimal parameters of conformal cooling channel, the structure can be further optimized using multiscale thermomechanical topology optimization, to obtain a lighter lattice injection mold without compromising the mechanical and thermal performance. The proposed approach involves structures in two scales: mesoscale and macroscale. In the mesoscale, lattice unit cells are analyzed in order to homogenize their thermomechanical properties. These properties are used in the macroscale where the lattice unit cells are optimally distributed. The macroscale design problem addressed in this work is to find the optimal distribution of given number of lattice phases within the component so its mass is minimized while satisfying stiffness and heat conduction constraints of the overall component and the specific regions. The approach is developed from our previous work[15].

4.1. Mesoscale material analysis

In the mesoscale, the elasticity tensor and thermal conductivity tensor for the cubic lattice structures are derived using asymptote homogenization method. The detail of this method can be seen in [6]. In this study, 10 functionally graded cubic lattice unit cells are analyzed. Since the structure is symmetric and orthotropic, only three components in the elasticity tensor (C_{1111}, C_{1122} and C_{1212}) and one component in the thermal conductivity tensor are required to be analyzed. The properties are interpolated using polynomial interpolation, and will be used in following thermomechanical topology optimization.

4.2. Thermomechanical topology optimization

The proposed thermomechanical topology optimization consists of two step. The objective of the first step is to find the optimized structure that minimize the mass, subjected to mechanical and thermal compliance, while satisfying the governing equations of the FEA models:

$$\begin{aligned} &\text{find } \boldsymbol{\theta}_1^* \in \mathbb{R}^{nc} \\ &\min\ J_1(\boldsymbol{\theta}_1) = m(\boldsymbol{\theta}_1)/m(\boldsymbol{\theta}_0) \\ &\text{subject to } W(\boldsymbol{\theta}_1) = \mathbf{f}^{\mathrm{T}}\,\mathbf{u}(\boldsymbol{\theta}_1) \le C_w\, W(\boldsymbol{\theta}_0) \\ &\qquad Q(\boldsymbol{\theta}_1) = \mathbf{q}^{\mathrm{T}}\,\mathbf{T}(\boldsymbol{\theta}_1) \le C_T\, W(\boldsymbol{\theta}_0) \\ &\qquad \boldsymbol{\theta}^{min} \le \boldsymbol{\theta}_1 \le \boldsymbol{\theta}^{max} \\ &\text{Satisfying } \mathbf{u}(\boldsymbol{\theta}_1) = \mathbf{K}(\boldsymbol{\theta}_1)^{-1}\mathbf{f} \\ &\qquad \mathbf{T}(\boldsymbol{\theta}_1) = \mathbf{K}_t(\boldsymbol{\theta}_1)^{-1}\mathbf{q}, \end{aligned} \tag{9}$$

where nc represents the number of unit cells; $\boldsymbol{\theta}_0$ represents the initial solid structure, $\boldsymbol{\theta}_1$ represents the optimized structure; W represents the mechanical compliance, where $\mathbf{f}$ is the nodal external force and $\mathbf{u}$ is the displacement caused by the nodal force; Q represents the thermal compliance, where $\mathbf{q}$ is the nodal heat flux and $\mathbf{T}$ is the temperature caused by the nodal heat flux; ; $\boldsymbol{\theta}^{min}$ represents the minimum volume fraction of the unit lattice cells, $\boldsymbol{\theta}^{max}$ represents the maximum volume fraction; $\mathbf{K}$ is the mechanical stiffness matrix, $\mathbf{K}_t$ is the thermal stiffness matrix. C_w and C_T are coefficients defined by designer that used to controlling the compromising of compliance. C_w can be a number greater than one, but if C_w is too large, the maximum stress of the structure may be

beyond allowed stress. C_T can be a number close or equal to one, to ensure the thermal performance is not decrease or only has a ignorable decrease. In this step, a linear interpolation of homogenized properties which only considering $\boldsymbol{\theta}^{min}$ and $\boldsymbol{\theta}^{max}$ can be used to ensure the problem is a convex problem having a global optimum.

Then, a fully constrained problem is solved in second step. Four additional constraints are needed to be added to the problem statement. First, the maximum displacement $U(\boldsymbol{\theta}_2)$ of the mold surface in contact with the injected part (Γ_1 and Γ_2) is required to be constrained to ensure the quality of the injected part. Besides, the maximum surface temperature in Γ_1 and Γ_2 are constrained to ensure the thermal performance is not decrease. These two constrained are written in the following equation:

$$\begin{aligned} U(\boldsymbol{\theta}_2) &= \max\{u_j(\boldsymbol{\theta}_2)\} \le U^{max}(\boldsymbol{\theta}_0)\ on\ \Gamma_1\ and\ \Gamma_2 \\ T(\boldsymbol{\theta}_2) &= \max\{u_j(\boldsymbol{\theta}_2)\} \le T^{max}(\boldsymbol{\theta}_0)\ on\ \Gamma_1\ and\ \Gamma_2 \end{aligned} \tag{10}$$

Additionally, the objective function is also modified to avoid mesh dependency and highly varied densities in order to create a multiphase material distribution that can be efficiently mapped to a manufacturable lattice structure. A gradient control regulation function

$$R(\boldsymbol{\theta}_2) = \sum_{c=1}^{nc} \nabla\theta_c^T\, \nabla\theta_c \tag{11}$$

is added to the objective to provide a mesh-independent result and improve the manufacturability, where $\nabla\theta_c$ is the spatial gradient of the design variable filed evaluated at the discrete cell. The intermediate densities caused by the addition of regularization function are clustered using

$$P(\boldsymbol{\theta}_2) = \sum_{c=1}^{nc} \prod_{p=1}^{np} \left|\theta_c - \theta_p^*\right|, \tag{12}$$

where θ_p^* are predefined relative density values. A small value $P(\boldsymbol{\theta}_2)$ ensures the design can be represented by a discrete number of unit cell phases np . Finally, the problem statement for the second step is

$$\begin{aligned} &\text{find } \boldsymbol{\theta}_1^* \in \mathbb{R}^{nc} \\ &\min\ J_1(\boldsymbol{\theta}_2) = \frac{m(\boldsymbol{\theta}_2)}{m(\boldsymbol{\theta}_0)} + C_R R(\boldsymbol{\theta}_2) + C_P P(\boldsymbol{\theta}_2) \\ &\text{subject to } W(\boldsymbol{\theta}_2) = \mathbf{f}^{\mathrm{T}}\, \mathbf{u}(\boldsymbol{\theta}_2) \le C_w\, W(\boldsymbol{\theta}_0) \\ &\qquad Q(\boldsymbol{\theta}_2) = \mathbf{q}^{\mathrm{T}}\, \mathbf{T}(\boldsymbol{\theta}_2) \le C_T\, W(\boldsymbol{\theta}_0) \\ &\qquad \text{Eq. (10)} \\ &\qquad \boldsymbol{\theta}^{min} \le \boldsymbol{\theta}_2 \le \boldsymbol{\theta}^{max} \\ &\text{Satisfying } \mathbf{u}(\boldsymbol{\theta}_1) = \mathbf{K}(\boldsymbol{\theta}_2)^{-1}\mathbf{f} \text{ and } \mathbf{T}(\boldsymbol{\theta}_1) = \mathbf{K}_t(\boldsymbol{\theta}_2)^{-1}\mathbf{q} \end{aligned} \tag{13}$$

The polynomial interpolation of the homogenization properties are used in the second step. The results can be obtained by solving this two-step problem using commonly used gradient based solver such as MMA.

4.3. Thermomechanical topology optimization Results

The optimized multi-phases structures for the cavity and the core are obtained using proposed method. The mechanical and thermal FEA models are similar with the models used in the optimization of conformal cooling. The difference is the dimension of the design domain. Considering the cost and benefits issue, we propose to optimize the smaller inserts containing the conformal cooling channels, then using press-fit technology to fit it to frames that can be easily manufactured using machining technology. The dimension of the cavity insert is 10.43cm×10.43cm×5.4864cm, and the dimension of the core insert is 10.43cm×10.43cm×5.7404cm and the core insert is 2.032cm. Thus total clamping load for the cavity insert is -0.91 kN and the clamping load for the core is 0.55 kN.

Three given phases of lattice unit cells are used to generate the lattice structures, which have volume fraction 1 (solid phase), 0.741 (medium lattice phase) and 0.259 (sparse lattice phase). The accepted optimal cavity is a 3-phases structure, shown in Fig.9. The three phases structure is preferred compared to two phases structure since it has smaller maximum Von Mises stress, which is 447 MPa. The Von Mises stress distribution, displacement distribution and temperature distribution of the optimal design is shown in Fig. 10. For the cavity, 17.25% mass is saved by using lattice structure.

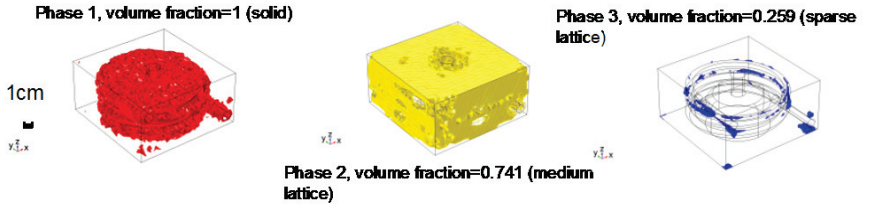

Fig. 9: Three lattice phases design for the cavity insert.

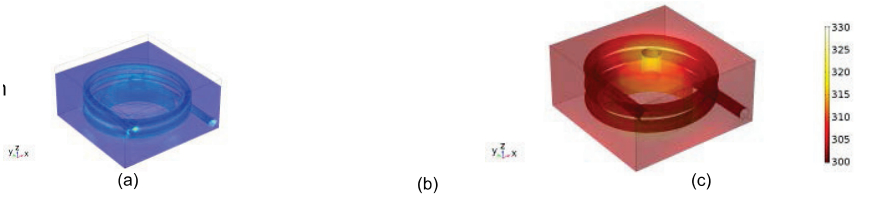

Fig. 10: (a) the von Mises stress, (b) total displacement and (c) temperature of the optimized cavity insert.

The accepted optimal core is a 2-phases structure, shown in Fig.11. For core, both of 2-phases and 3-phases structure are valid, the 2-phases structure is preferred since it saving more mass. The Von Mises stress distribution, displacement distribution and temperature distribution of the optimal design is shown in Fig. 12. For the core, 37% mass is saved by using lattice structure.

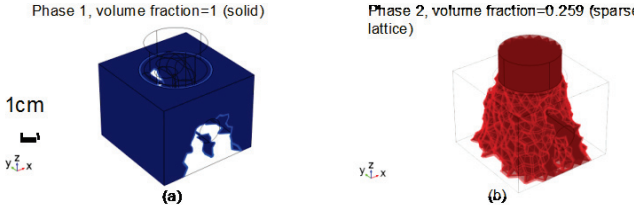

Fig. 11: Two lattice phases design for the cavity insert.

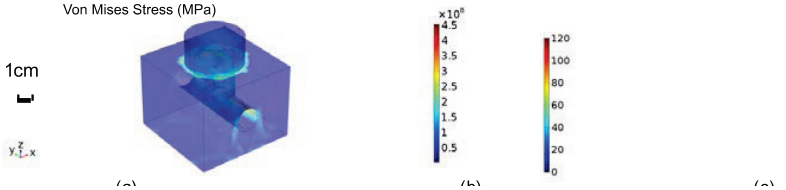

Fig. 12: (a) the von Mises stress, (b) total displacement and (c) temperature of the optimized core insert.

5. Prototyping and the manufacturability

Prototypes of the final lattice designs of the cavity and the core inserts with conformal cooling channels are 3D printed using a stereolithography unit (Formlabs Form 2, Somerville, Massachusetts). Clear resin is used to visualize the internal lattice structure and conformal cooling channels (Fig. 13 (a) and (d)). The lattice cube size is 5 mm with a minimum member size of 1.7 mm. No internal support structure is required. In order to demonstrate the feasibility to 3D print in metal using PBF, a sample containing 125 graded lattice cubes (5×5×5) is designed and printed in a PBF unit (EOS M280, Hamburg, Germany) as shown in Fig. 13 (g). Each lattice cube size is 5mm. No internal support structure is used in the 3D-printing process. The test shows that, without internal structure, the quality of any lattice cube with minimum member size (the size the lattice bars) of and hole size (the size of the distance

between two lattice bars) greater than 0.03 in (0.0762 mm) is guaranteed. This sample may prove the optimal design can be printed by this PBF unit without internal structure. Besides, we prepared samples printed by PBF which will be tested to determine the accurate value of mechanical and thermal properties for the material (Fig. 13 (h)). The test is still ongoing, and the coming results will be used to calibrate the simulation model.

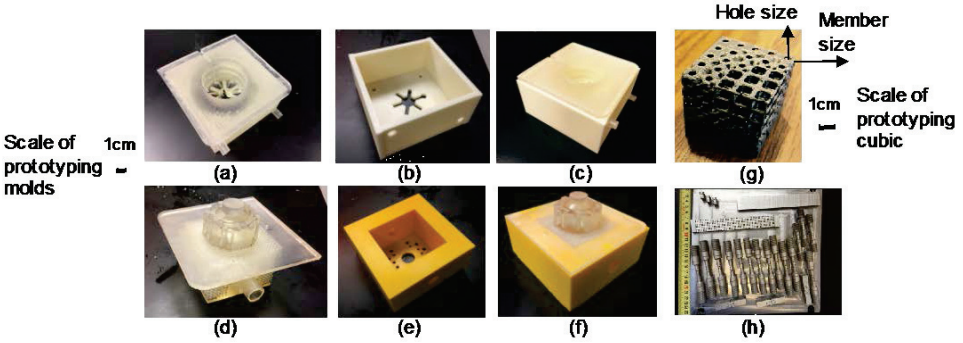

Fig. 13: (a) the cavity insert, (b) cavity frame and (c) press-fitted cavity plate; (d) The core insert (e) core frame and (f) press-fitted core plate. (g) a sample containing 125 graded lattice cubes printed in a PBF unit, (h) samples printed for further experiment to determine the material properties and to calibrate the simulation models.

6. Conclusion

In this work, a new approach of design optimization of plastic injection tooling (mold) is presented. This approach concerns both thermal and mechanical performance of an injection mold. Using the proposed approach, the structure is represented by a given unit lattice cell phases, which facilitate the additive manufacture process such as stereo-lithography (SLA) and power bed fusion (PBF).

The optimization procedure consists of a parameter optimization based on thermomechanical finite element model, and a multiscale thermomechanical topology optimization. In the parameter optimization, finite element analysis is treated as black-box functions which can be optimized by using derivative-free methods. Thermomechanical properties of lattice unit cells are derived using asymptotic homogenization and interpolated in mesoscale, to conduct the macroscale structural optimization problem which can be solved through thermomechanical topology optimization.

This study has some limitations that required to be improved in the future work. First, field test for the stainless steel used in DMLS is ongoing and the properties for optimization will be updated. Second, the final STL requires further detail CAD repair to fulfill the requirement of PBF. In the near future, the model will be manufactured in PBF, and the thermal and mechanical performance will be validated by conducting experiments.

Acknowledgements

The Walmart Foundation supported this research effort. Hewitt Molding Company provided the original injection mold model for the investigation. Any opinions, findings, conclusions, and recommendations expressed in this investigation are those of the writers and do not necessarily reflect the views of the sponsors.

References

[1] A. Equbal, A. Sood, and M. Shamim, "Rapid tooling: A major shift in tooling practice," *Journal of Manufacturing and Industrial Engineering*, vol. 14, pp. 1-9, 2015.

[2] T. Wu, S. A. Jahan, P. Kumaar, A. Tovar, H. El-Mounayri, Y. Zhang, *et al.*, "A framework for optimizing the design of injection molds with conformal cooling for additive manufacturing," *Procedia Manufacturing*, vol. 1, pp. 404-415, 2015.

[3] D. O. Kazmer, *Injection mold design engineering*: Carl Hanser Verlag GmbH Co KG, 2016.

[4] J.-H. Choi, S.-H. Choi, D. Park, C.-H. Park, B.-O. Rhee, and D.-H. Choi, "Design optimization of an injection mold for minimizing temperature deviation," *International Journal of Automotive Technology*, vol. 13, pp. 273-277, 2012.

[5] C. Ramos, P. Carreira, P. J. Bártolo, and N. Alves, "OPTIMALMOULD| Cooling System Influence in Injection Moulding Cycle Time Optimization," in *Advanced Materials Research*, 2013, pp. 544-547.

[6] E. Andreassen and C. S. Andreasen, "How to determine composite material properties using numerical homogenization," *Computational Materials Science*, vol. 83, pp. 488-495, 2014.

[7] A. T. Gaynor, N. A. Meisel, C. B. Williams, and J. K. Guest, "Multiple-material topology optimization of compliant mechanisms created via PolyJet three-dimensional printing," *Journal of Manufacturing Science and Engineering*, vol. 136, p. 061015, 2014.

[8] T. Gao, W. Zhang, J. Zhu, Y. Xu, and D. Bassir, "Topology optimization of heat conduction problem involving design-dependent heat load effect," *Finite Elements in Analysis and Design*, vol. 44, pp. 805-813, 2008.

[9] W. J. Sames, F. List, S. Pannala, R. R. Dehoff, and S. S. Babu, "The metallurgy and processing science of metal additive manufacturing," *International Materials Reviews*, vol. 61, pp. 315-360, 2016.

[10] Y. Zhang and J. Zhang, "Sintering phenomena and mechanical strength of nickel based materials in direct metal laser sintering process—a molecular dynamics study," *Journal of Materials Research*, vol. 31, pp. 2233-2243, 2016.

[11] K. Kunze, T. Etter, J. Grässlin, and V. Shklover, "Texture, anisotropy in microstructure and mechanical properties of IN738LC alloy processed by selective laser melting (SLM)," *Materials Science and Engineering: A*, vol. 620, pp. 213-222, 2015.

[12] D. Lee and M. Wiswall, "A parallel implementation of the simplex function minimization routine," *Computational Economics*, vol. 30, pp. 171-187, 2007.

[13] M. J. Powell, "A direct search optimization method that models the objective and constraint functions by linear interpolation," in *Advances in optimization and numerical analysis*, ed: Springer, 1994, pp. 51-67.

[14] S. Yoo and D. F. Walczyk, "A preliminary study of sealing and heat transfer performance of conformal channels and cooling fins in laminated tooling," *Journal of manufacturing science and engineering*, vol. 129, pp. 388-399, 2007.

[15] T. Wu, K. Liu, and A. Tovar, "Multiphase Thermomechanical Topology Optimization of Functionally Graded Lattice Injection Molds," in *ASME 2016 International Design Engineering Technical Conferences and Computers and Information in Engineering Conference*, 2016, pp. V02AT03A036-V02AT03A036.